Docking and pharmacophore mapping of halogenated pyridinium derivatives on heat shock protein 90

Mahmoud A. Al-Sha'er[a]*, Iman Mansi[b] and Nancy Hakooz[a]

[a]Faculty of Pharmacy, Zarqa University, Zarqa, Jordan
[b]Faculty of Pharmaceutical sciences, Hashemite University, Zarqa, Jordan

_____

ABSTRACT

Based on previous studies on pyridinium derivatives as heat shock protein (hsp90) inhibitors, we explored the pharmacophoric features by measuring the inhibitory effect of synthetic halogenated pyridinium derivatives on hsp90 ATPase site, followed by mapping of the synthetic compounds on successful hypotheses; Hypo1/7 Hypo8/8 and Hypo9/1 previously modelled, then docking of the synthetic compounds on geldanamycin binding site of hsp90 protein 1YET. The inhibition of ATPase activities of hsp90 was measured and expressed as percentage of inhibition for 77 pyridinium derivatives with variable substituent. The highest percentage of inhibition was found for compounds 34, 16 and 48, equal to 48.12% , 42.67% and 40.72% related to 4-bromo-4-flouro-pyridinium derivative , 3-chloro-4-flouro-pyridinium derivative and 4-methylsulfide-4-bromo-pyridnium derivative respectively. Grid based model and 3D QSAR analysis indicate the importance of Van der Waal interaction and electrostatic potential in determining hsp90 inhibition.

Keywords: Pyridinium derivatives, Hsp90, Cancer, Pharmacophore, Docking

_____

INTRODUCTION

Heat shock protein 90 (Hsp90) belongs to a family of molecular chaperones that play a pivotal role in the conformational maturation, stability, and functions of protein substrates within the cell. The ATPase activity of Hsp90α provides the energy needed to refold denatured cellular proteins [1]. Amongst the client proteins of Hsp90α are many oncogenes that are essential for the survival, proliferation, invasion, metastasis, and angiogenesis of tumors [2]. In fact, several oncogenic proteins have been shown to be dependent upon Hsp90α for conformational activation, including telomerase, Her2 (erbB2), Raf-1, focal adhesion kinase, and steroid hormone receptors [3]. The validity of Hsp90α as an anticancer target for drug discovery [4,5] was further established by emerging clinical and preclinical trials employing the potent Hsp90α inhibitor 17-allylamino-17-desmethoxygeldanamycin as well as the natural Hsp90α inhibitors geldanamycin [6], radicicol [7], and other small molecules [8]. The significance of heat shock protein (Hsp90) as a target in anticancer research [1–5, 9–14], combined with the availability of appropriate crystallographic structures for this target [15,16], prompted us to apply computational technique-docking-based, pharmacohore mapping, multiple linear regression analysis (MLR) [17]—to this target, aiming at the discovery of new pyridinium Hsp90α inhibitors. Molecular docking, which is basically a conformational sampling procedure in which various docked conformations are explored to identify the right one, can be a very challenging problem given the degree of conformational flexibility at the ligand-macromolecular level [18–20]. Docking programs employ diverse methodologies to evaluate different ligand conformations within binding pockets, [21–30], but they must be guided by scoring functions when evaluating the fit between the protein and the corresponding docked ligand(s) [31–37]. The underlying ligand–receptor molecular interactions are highly complex, and various terms should be considered when quantifying the free energy of the interaction process [38].

_____

Importance of hetero cyclic compounds has long been recognized in the field of synthetic organic chemistry. It is well known that heterocyclic compounds containing nitrogen and sulphur exhibit a wide variety of biological activity [39]. A series of pyridine derivative were evaluated for antitumor activities [40]. Nicotinamide has been shown to be beneficial in the treatment of papular and pustular acne, as well as improvement of skin cancer [41]. Nicotinamide or nicotinic acid has been used to treat diseases such as hyper-cholesterolemia and schizophrenia [42,43]. Nicotinamide and its derivatives are also used to prevent type-1 diabetes in animal model and humans showed cytotoxic properties [44,45]. On other hand 6–chloro–3-substituted pyridine are very important class of heterocycles and are widely used in pharmaceutical and agrochemical industry [46]. The increasing interest in the chemistry of nicotinamide and its substituted derivatives result from the wide possibilities and their practical application for obtaining biologically active agents. Derivatives of S-protected triazole and diazole exhibit high anti-inflammatory activity [47]. Previously synthesized pyridinium derivatives showed hsp90 inhibitory effect [48]. Our interest is to explore the hsp90 inhibition of new halogenated pyridinium derivatives. An attempt has been made to understand the structural activity relationship of hsp90 inhibitory effect of pyridinium derivatives [48-50].

EXPERIMENTAL SECTION

2.1 *In vitro* Experimental Studies
2.1.1. Reagents and Reference Samples
Active hsp90 enzyme 10 □g (Sigma-Aldrich, Germany), malachite green 99% (Sigma-Aldrich, Germany), Ammonium molybdate 95% (Sigma-Aldrich, Germany), Sodium citrate 99% (Sigma-Aldrich, Germany), ATP 1mM solution (Sigma-Aldrich, Germany), Allylaminogeldanamycin 10 mg (Sigma-Aldrich, Germany), 77 Synthetic pyridinium derivatives purified and analyzed (Faculty of Pharmacy, Zarqa University).

2.1.2 Preparation of hit compounds for *In vitro* assay
The tested compounds were provided as dry powders in variable quantities (5-500 mg). They were initially dissolved in DMSO to give stock solutions of 0.02 M. Subsequently, they were diluted to the required concentrations with deionized water for enzymatic assay.

2.1.3 Quantification of hsp90 activity in a spectrophotometric assay
The ATPase activity of hsp90 was quantified by colorimetric measurement of released inorganic phosphate [51]. Bioassays were performed as follows; in a 96-well clear plate, the reaction solution of total volume of 50μL contains 100mM Tris/HCl, pH 7.4, 6mM MgCl2, 20mM KCl, 100μM ATP, 0.1mg/ml BSA and 50ng/well of human hsp90 enzyme, 5 μL of tested compounds. The plate was sealed and the reaction was incubated at 37°C for 24 hours. The reaction was stopped by the addition of 50μL of previously prepared malachite green solution (5.2% ammonium molybdate in H2SO4, 0.0812% malachite green, 2.32% polyvinyl alcohol and water in ratios of 1:2:1:2 respectively), followed by 10 μL of 10% Sodium citrate, left for 20 minutes and the absorbance at 630 nm was measured using a plate reader (Bio-Tek instruments ELx 800, Winooski, VT). The calibration curve was prepared using 5 different concentrations of phosphate ion (10-200μM). The final concentration of DMSO did not exceed 1.0%. Inhibition of hsp90 was calculated as percent activity of the uninhibited ATPase control. Allylaminogeldanamycin [52] was tested as positive control, while negative controls were prepared by adding the substrate after reaction termination.

2.2 Docking
The 3D coordinates of hsp90 were retrieved from the Protein Data Bank (Hsp90, PDB code: 1YET, resolution: 1.9 Å). Hydrogen atoms were added to the protein, utilizing DS 4.0 templates for protein residues. Libdock algorithm was used within DS 4.0. In the current docking experiments, the binding site was generated from the co-crystallized ligand (geldanamycin, GMD), and pyridinium compounds were docked into the binding site [53].

2.3 Pharmacophore mapping
The screened compounds were mapped against hsp90 pharmacophoric models [54]; Hypo1/7, Hypo8/8 and Hypo9/1 using ligand pharmaophore mapping module in discovery studio DS 4.0 [55].

RESULTS AND DISCUSSION

Previously synthesized pyridinium derivatives showed hsp90 inhibitory effect [48]. Accordingly, we initiated an exploratory effort to evaluate a series of pyridinium-based compounds exemplified by synthetic compounds **1-77** [50] (table 1, figure 1). Our interest is to explore the pharmacophoric features

of heat shock protein (Hsp90) inhibitor using malachite green assay [51]. In addition to comparision of the docking pose [53] with the way of mapping [54,55].

Table 1 shows the tested compounds (**1**-**77**), which have been previously synthesized [50], it summarizes the fit values for both Hypo1/7, Hypo8/8 and Hypo9/1, in addition to percentage of ATPase inhibition of hsp90 at 100□M. However, the mapping with pharmacophores is almost not similar between the pyridinium derivatives and can not alone explain the variable hsp90 inhibition, e.g. hypo1/7 shows the highest fit while hypo8/8 failed to map any compound, other factors interfer with the activity ; variable two dimensional discriptors such as AlogP [56], molecular weight, number of hydrogen bond acceptors inversly affect the model while ECFP_6 [56] fragment , fitting with pharmacophores Hypo1/7 and Hypo9/1 positively affect the model as shown by MLR analysis in equation 1:

[MLRTempModel] = 5.906 - 34.53 x [ALogP] - 0.1045 x [Molecular_Weight] - 9.728 x
[Num_H_Acceptors] + 5.871 x [ECFP_6] + 4.138 x [Hypo9/1] + 2.195 x [Hypo1/7] ……………Eq1
N= 77 　 , 　　　　　　　R^2 = 0.416, 　　　　　　　q^2 (cross validation) = 0.006

Furthermore by building 3DQSAR model (R^2 = 0.719) that create grid based model using DS 4.0 as shown in figure 3B and figure 4. It is clear from the analysis; the contribution of Van der Waal interactions and electrostatic potential of the substituent in explaining the structure activity relationship of pyridinium derivatives. However, all of them have the same scaffold but change in the substituent at R_1, R_2, R_3, R_4 groups by lipophilic functional groups with variable lipophilicity and molecular size. Although mapping with Hypo1/7 is almost higher than fitting with Hypo9/1 and similar between all pyridinium derivatives , it could not explain the activity alone. It is clear that mapping with pharmacophores alone is unnecssarily lead to active compounds, the physicochemical properties such as lipophilicity, molecular volume , electrostatic potential and Van der Waal interactions play a signifcant role in determining the structure activity relationship of tested compounds. Further exploration of the molecular interaction of potential pyridinium compound **34** (% inhibition = 48.1%) , as shown in figure 1, (A, B, E) that show mapping with Hypo1/7, Hypo9/1 and pose of docked compound **34** inside the binding pocket of hsp90 (pdb: 1 YET) after docking inside the ATPase binding site of hsp90 using libdock module in DS 4.0, the corresponding amino acids that are involved in the interactions significantly are; Lys58, Asn51, Phe138, Leu107, Asp102, Lys112, Asp93 and Met98. Those amino acids form the binding pocket for the corresponding docked compounds. By comparision the mapping features in (A) Hypo1/7 that could be explained as follows; bromo atom mapped with hydrophobic feature corresponding to Van der Waal interaction with hydrophobic part of Val136 , Lys112, and mapping corresponding phenyl group with ring aromatic feature is due to pi stacking of electron rich aromatic group of Phe138 with electron poor aromatic group in compound **34**. Two Hydrogen bond donors corresponding to interaction of NH groups with two carbonyl group of Asn51. Furthermore, mapping compound **34** with Hypo9/1 as shown in Fig.1 (B) correlated with the docking pose inside the geldanamycin binding pocket of hsp90 (coded 1YET, resolution 1.9A); flouro group mapped with hydrophobic feature correspoding to Van der Waal interaction with hydrophobic part of Lys58. Mapping phenyl group with ring aromatic feature is corresponding to pi stacking with Met98 according to figure 1E, two hydrogen bond donors corresponding to interaction of NH groups of pyridinium compound with corresponding two carbonyl groups of Asn51. Two dimensional analysis of docked pose of compound **34** inside the binding pocket of hsp90 (pdb: 1YET, resolution 1.9A) using the function (Analyze single complex) in Discovery Studio DS 3.5 was used as shown in figure 2A. It is clear that several types of interactions with corresponding amino acids in the binding pocket such as; Ile96, Ala55, Gly97, Ser52, Thr184, Asn106, Tyr139, and Asn106 corresponding to hydrophobic interactions , Gly135, Met98, Lys58 and Asn51 corresponding to electrostatic interactions. However, figure 1 (E) shows the most important amino acids that correlated with the mapped features in Hypo1/7 and Hypo9/1. Figure 2A,B shows extra amino acids that is involved in the interactions. It is known that not all interactions inside the binding pockets are important for activity, docking lack the connection of activity with docked pose [57], however the docked poses are scored by several functions that are not necessarily correlated with activity [53] Figure 3B shows the two dimensional plot of 3DQSAR model that correlates the GridBasedTempModel with the percentage of inhibition values for 77 pyridinium compounds linearly. GridBasedTemp Model is dependent on two parameters; Van der Waal (VDW) values and electrostatic potential (EP) values as represented in figure 4. The MLR analysis in equation 1 explains the correlation of most important discriptors that affect the hsp90 ATPase inhibition by pyridinium compounds **1**-**77**.

Table 1: Pyridinium derivatives with percentage of hsp90 inhibition
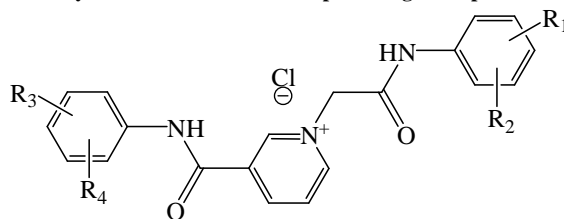
No	R_1	R_2	R_3	R_4	Hypo1/7	Hypo8/8	Hypo9/1	% Inhibition*
1	4-Cl	H	4-Cl	H	8.399	0	3.888	3.84
2	4-Cl	H	3-Cl	H	8.838	0	4.942	10.48
3	4-Cl	H	2-Cl	H	8.904	0	4.161	25.53
4	4-Cl	H	4-Br	H	8.905	0	4.469	5.51
5	4-Cl	H	4-I	H	8.797	0	4.007	8.67
6	4-Cl	H	4-CH3S-	H	8.885	0	3.678	10.71
7	4-Cl	H	4-F	H	8.824	0	4.384	12.44
8	4-Cl	H	2-Cl	4-Cl	8.907	0	4.115	16.95
9	4-Cl	H	3-Cl	5-Cl	8.911	0	4.857	20.86
10	3-Cl	H	4-Cl	H	8.558	0	5.033	12.50
11	3-Cl	H	3-Cl	H	7.049	0	4.96	19.11
12	3-Cl	H	2-Cl	H	6.845	0	4.964	9.16
13	3-Cl	H	4-Br	H	8.295	0	4.574	5.72
14	3-Cl	H	4-I	H	8.29	0	4.58	32.52
15	3-Cl	H	4-CH3S-	H	8.522	0	4.961	27.01
16	3-Cl	H	4-F	H	6.859	0	4.906	42.67
17	3-Cl	H	2-Cl	4-Cl	8.517	0	4.972	14.95
18	3-Cl	H	3-Cl	5-Cl	8.973	0	4.83	19.13
19	2-Cl	H	4-Cl	H	8.489	0	4.094	0
20	2-Cl	H	3-Cl	H	7.029	0	4.928	16.41
21	2-Cl	H	2-Cl	H	3.771	0	3.715	0
22	2-Cl	H	4-Br	H	8.331	0	3.837	17.50
23	2-Cl	H	4-I	H	8.442	0	3.482	10.0
24	2-Cl	H	4-CH3S-	H	8.557	0	3.686	7.76
25	2-Cl	H	4-F	H	3.774	0	3.595	16.66
26	2-Cl	H	2-Cl	4-Cl	8.463	0	3.99	9.64
27	2-Cl	H	3-Cl	5-Cl	7.037	0	4.859	14.73
28	4-Br	H	4-Cl	H	8.974	0	4.29	19.88
29	4-Br	H	3-Cl	H	8.974	0	4.897	29.88
30	4-Br	H	2-Cl	H	8.977	0	4.104	8.72
31	4-Br	H	4-Br	H	8.987	0	4.148	26.20
32	4-Br	H	4-I	H	8.981	0	3.787	29.78
33	4-Br	H	4-CH3S-	H	8.968	0	4.138	13.10
34	4-Br	H	4-F	H	8.972	0	4.155	48.12
35	4-Br	H	2-Cl	4-Cl	9.021	0	4.325	10.83
36	4-Br	H	3-Cl	5-Cl	8.973	0	4.83	12.36
37	4-I	H	4-Cl	H	8.97	0	4.113	19.29
38	4-I	H	3-Cl	H	9.038	0	5.032	38.19
39	4-I	H	2-Cl	H	8.977	0	4.005	35.17
40	4-I	H	4-Br	H	9.038	0	3.826	21.14
41	4-I	H	4-I	H	9.032	0	3.669	12.39
42	4-I	H	H	4-CH$_3$S-	8.961	0	3.878	28.86
43	4-I	H	4-F	H	9.026	0	4.023	18.50
44	4-I	H	3-Cl	5-Cl	9.044	0	4.852	33.63
45	4-CH$_3$S-	H	4-Cl	H	8.9	0	4.486	15.47
46	4- CH$_3$S-	H	3-Cl	H	8.744	0	4.894	38.47
47	4- CH$_3$S-	H	2-Cl	H	8.74	0	4.498	18.26
48	4- CH$_3$S-	H	4-Br	H	8.862	0	4.348	40.72
49	4- CH$_3$S-	H	4-I	H	8.573	0	4.22	0
50	4- CH$_3$S-	H	4-CH3S-	H	8.717	0	4.005	2.04
51	4- CH$_3$S-	H	4-F	H	8.74	0	3.8	13.21
52	4- CH$_3$S-	H	2-Cl	4-Cl	8.9	0	4.486	0
53	4- CH$_3$S-	H	3-Cl	5-Cl	8.62	0	4.791	6.43
54	4-F	H	4-Cl	H	8.399	0	3.888	4.32
55	4-F	H	3-Cl	H	7.062	0	4.924	31.17
56	4-F	H	2-Cl	H	3.849	0	3.018	4.30
57	4-F	H	4-Br	H	8.609	0	3.609	35.40
58	4-F	H	4-I	H	8.342	0	3.514	16.63
59	4-F	H	4-CH$_3$S-	H	8.502	0	2.948	23.92
60	4-F	H	4-F	H	3.678	0	3.011	31.70
61	4-F	H	2-Cl	4-Cl	8.441	0	4.161	0
62	4-F	H	3-Cl	5-Cl	7.04	0	4.884	37.59
63	2-Cl	4-Cl	3-Cl	H	8.629	0	4.926	1.06
64	2-Cl	4-Cl	2-Cl	H	8.86	0	4.184	10.94

_____

65	2-Cl	4-Cl	4-Br	H	8.807	0	4.318	25.52
66	2-Cl	4-Cl	4-I	H	8.68	0	4.058	16.82
67	2-Cl	4-Cl	4-CH₃S-	H	8.885	0	4.848	22.77
68	2-Cl	4-Cl	2-Cl	4-Cl	8.877	0	4.129	8.44
69	2-Cl	4-Cl	3-Cl	5-Cl	8.885	0	4.848	28.53
70	3-Cl	5-Cl	4-Cl	H	8.548	0	4.691	16.61
71	3-Cl	5-Cl	3-Cl	H	7.048	0	4.906	3.53
72	3-Cl	5-Cl	2-Cl	H	6.871	0	5.244	0
73	3-Cl	5-Cl	4-Br	H	8.535	0	4.765	17.55
74	3-Cl	5-Cl	4-I	H	8.605	0	4.842	14.37
75	3-Cl	5-Cl	4-CH₃S-	H	8.521	0	4.921	0.3
76	3-Cl	5-Cl	4-F	H	6.884	0	4.699	8.89
77	3-Cl	5-Cl	2-Cl	4-Cl	8.487	0	5.317	20.57

* Inhibition at 100 micM concentration
AAG was used as standard inhibitor with 87% inhibition at 100micM

(**A**)

(**B**)

(**C**)

(**D**)

(E)   **(F)**
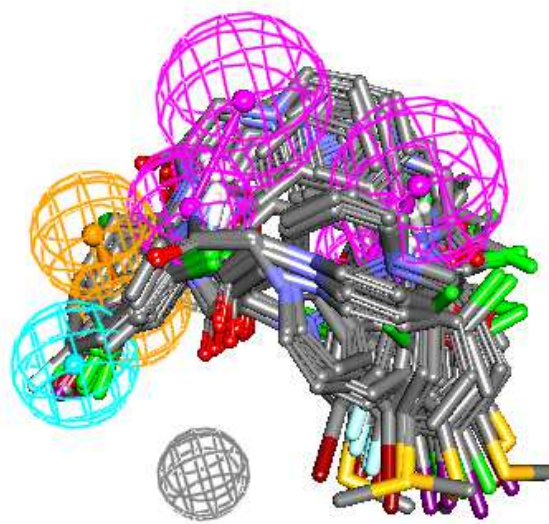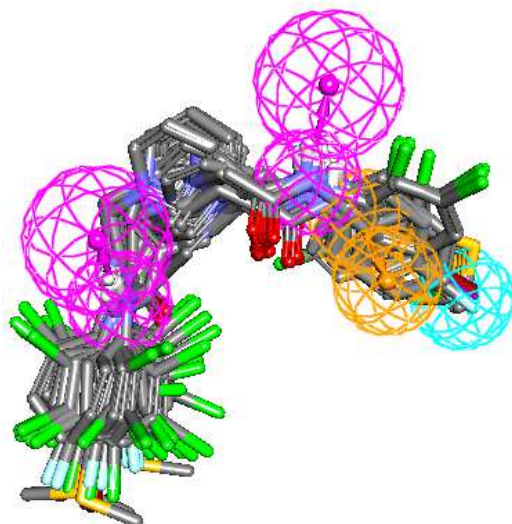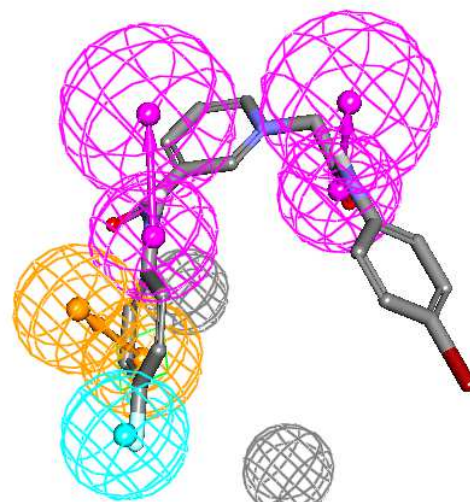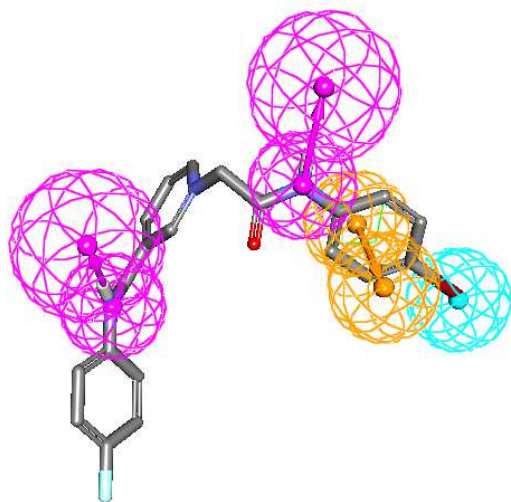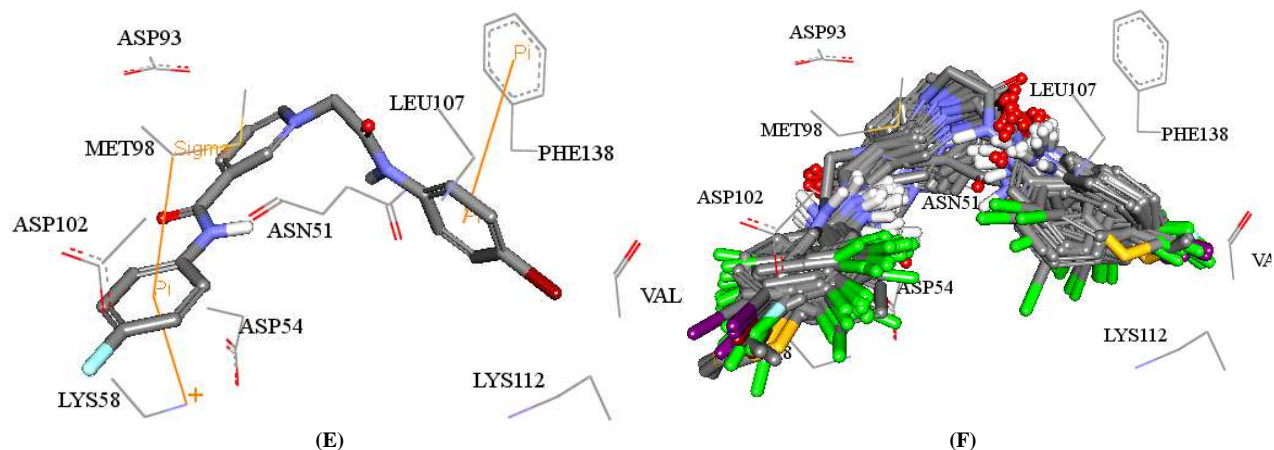
Figure 1 : (A)mapping of Hypo1/7 with compound 34, (B) mapping of Hypo9/1 with compound 34 (C) Mapping of Hypo1/7 with compounds 1-77, (D) mapping of Hypo9/1 with compounds 1-77, (E) Highest libDockScore pose of compound 34 docked inside the binding pocket of hsp90 (1YET, resolution 1.9A) (F) docked compounds 1-77 with highest libDockScore.

(A)
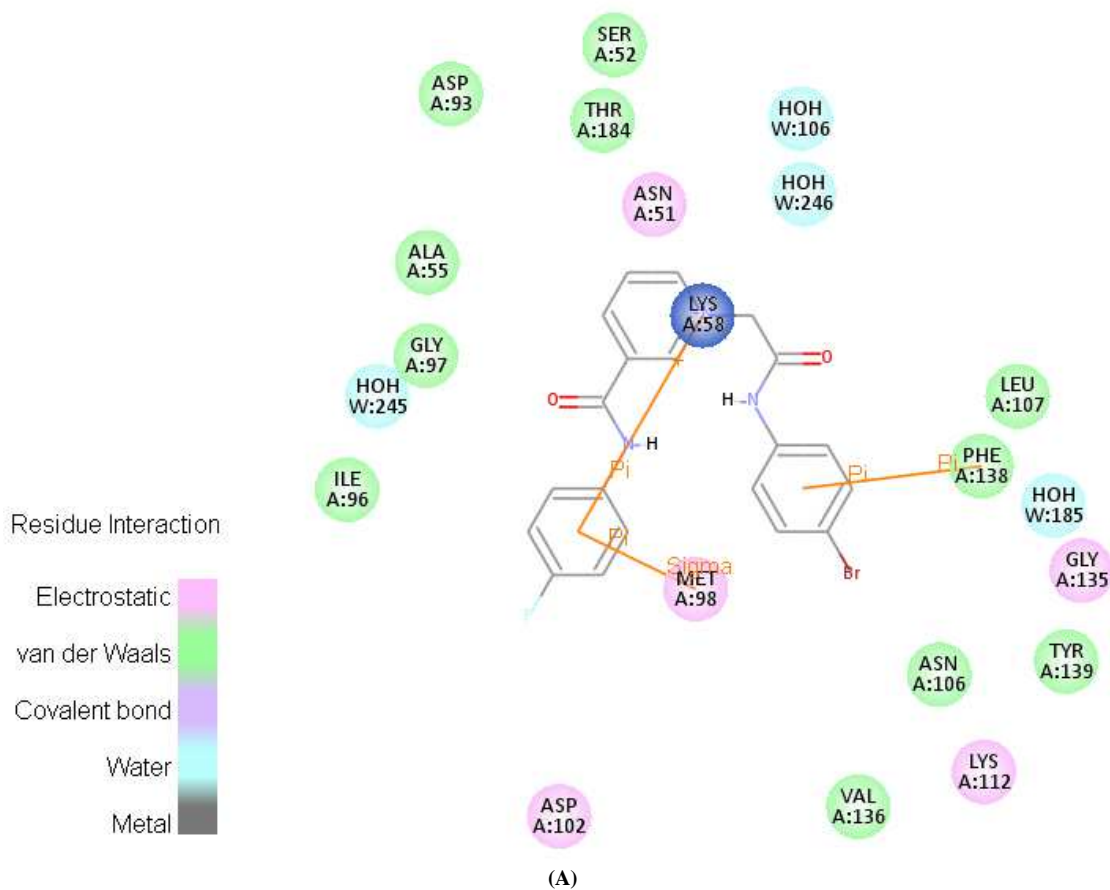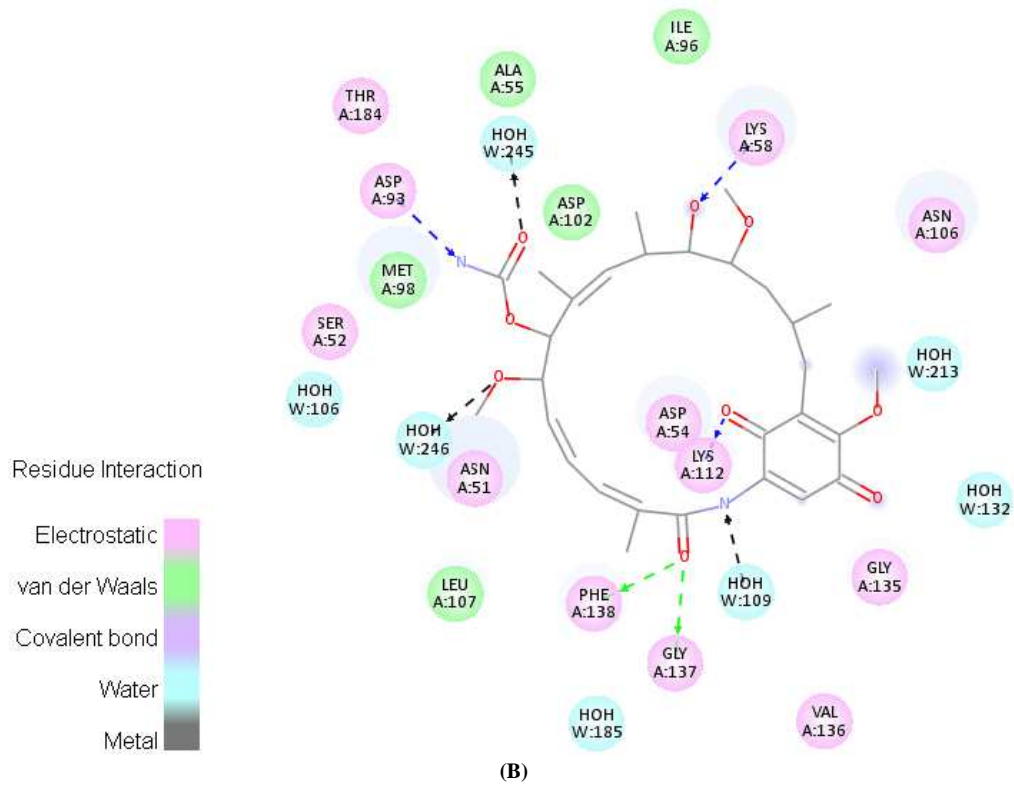
Figure 2: (A) Two dimensional analysis of the pose with highest libDockScore of compound 34 (B) Two dimensional analysis of the cocrystalized geldanamycin (1YET) using DS 3.5 visualizer

$$y = 0.416x + 9.749$$

R-square = 0.416
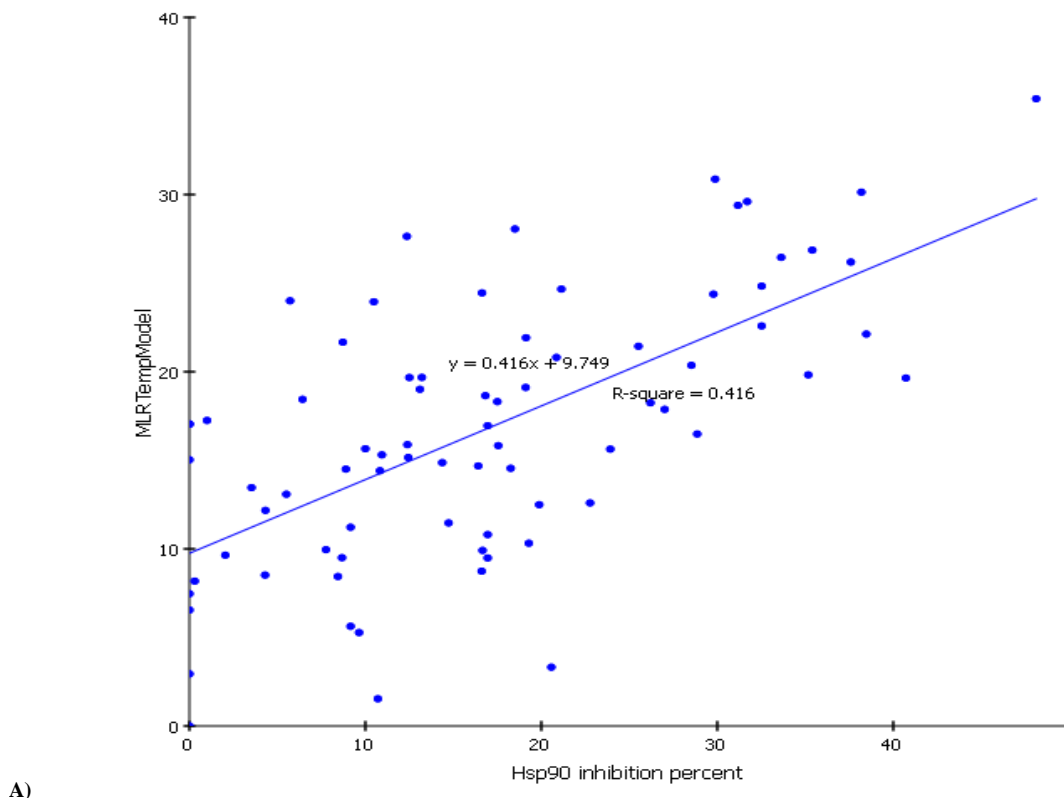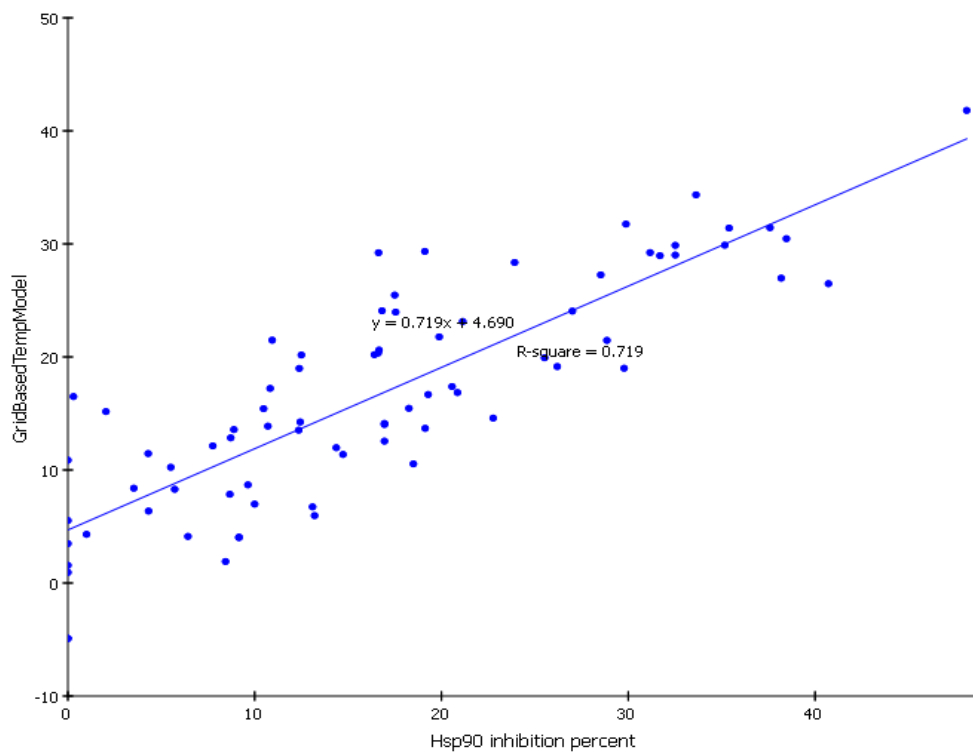
B)

Figure 3: Two dimensional plot of A) Multiple Linear Regression analysis (MLR) model that correlate the MLRTempModel with the percentage of inhibition for pyridinium compounds, B) 3DQSAR model that correlate the GridBasedTempModel with the percentage of inhibition for pyridinium compounds

(A)

_____

(B)
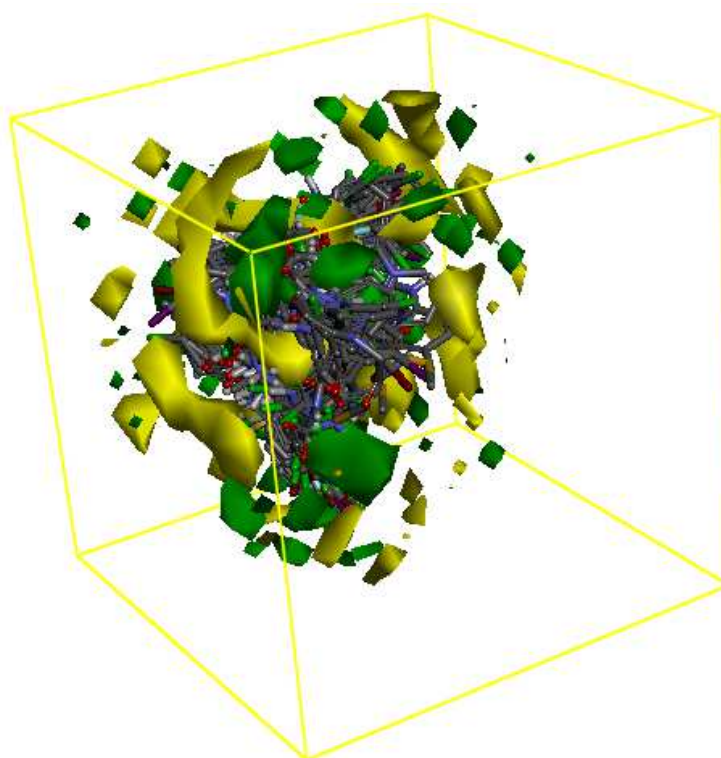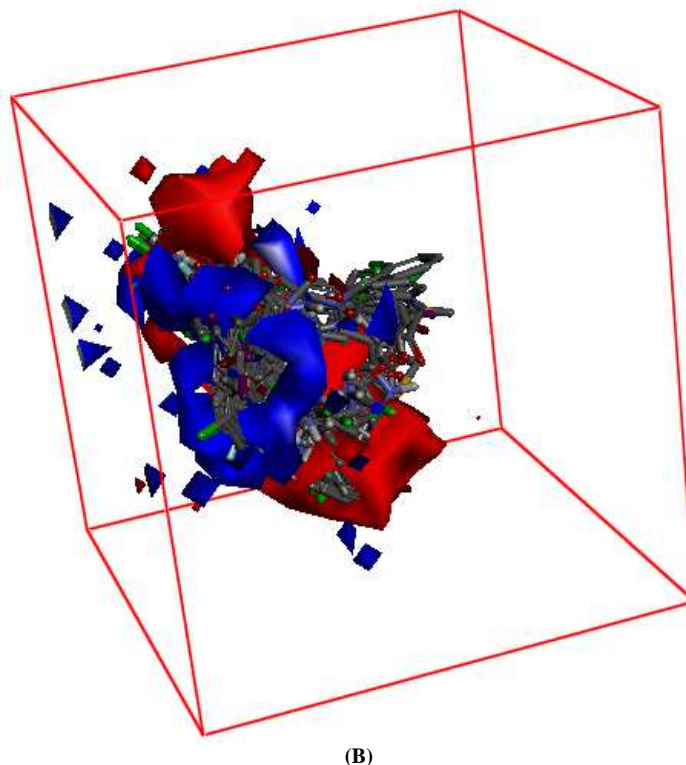
Figure 4: Grid Based Model of the pyridinium compounds aligned to (A) Van der Waal (VDW) model, yellow color means negative VDW Isosurface, green color means positive VDW Isosurface (B) Electrostatic potential (EP) model using DS 4.0., red color means negative EP Isosurface, blue color means positive EP Isosurface

CONCLUSION

Although effective mapping of pyridinium compounds with hsp90 hypotheses and successful docking inside the ATPase binding site, 3D-QSAR model, grid based model indicates the significance of the physicochemical properties; Van der Waal interaction and electrostatic potential in hsp90 inhibition of pyridinium scaffold.

REFERENCES

[1] D Mahalingam; R Swords; JS Carew; ST Nawrocki; K Bhalla; FJ Giles, *Br. J. Cancer* , **2009**, 100, 1523–1529
[2] G Chiosis; Rodina A; Moulick K, *Anti Cancer Agents Med. Chem*., **2006**, 6, 1–8.
[3] BW Dymock; MJ Drysdale; E McDonald; P Workman, *Expert Opin. Ther. Pat*., **2004**, 14, 837–847
[4] JS Isaacs; W Xu; L Neckers, *Cancer Cell*, **2003**, 3, 213–217
[5] LH Pearl; C Prodromou; P Workman, *Biochem. J.,* **2008**, 41, 439–453
[6] L Neckers; TW Schulte; E Mimnaugh, *Invest. New Drugs*, **1999**, 17, 361–373
[7] S Soga; Y Shiotsu; S Akinaga; SV Sharma, *Curr Cancer Drug Targets* , **2003**, 3, 359–369.
[8] G Chiosis; Y Kang; W Sun, *Expert Opin Drug Discov*., **2008**, 3, 99–114
[9] P Hwangseo; K Yun-Jung; H Ji-Sook , *Bioorg. Med. Chem. Lett* ., **2007**, 17, 6345–6349.
[10] X Barril; M Beswick; A Collier; M Drysdale; B Dymock; A Fink; K Grant; R Howes; A Jordan; A Massey, *Bioorg. Med. Chem. Lett.,* **2006**, 16, 2543–2548.
[11] X Barril; P Brough; M Drysdale; RE Hubbard; A Massey; A Surgenor; L Wright, *Bioorg. Med. Chem. Lett*. **2005**, 15, 5187–5191.
[12] G Chiosis; B Lucas; A Shtil; H Huezoa; N Rosen, *Bioorg. Med. Chem*., **2002**, 10, 3555–3564.
[13] L Neckers, *Curr. Top. Med. Chem.,* **2006**, 6, 1163–1171.
[14] L Xiao; X Lu; DM Ruden. *Mini-Rev. Med. Chem*.,**2006**, 6, 1137–1143.
[15] L Neckers; M Mollapour; S Tsutsumi, *Trends Biochem Sci* , **2009**, 34, 223–226.

_____

[16] RH Jeffrey; P Chang; MP Andrew; RK Aaron; DW Michael; W Xilu; LL Christopher; CM Jamey; MS Kerry; AJ Russell; C Jun; LR Paul; J Sha; KT Stephen; DM Edward; AD Sarah; SL Uri; MS Jean; AW Karl; MB Diane; WF Stephen; WE Steven; JH Philip, *Chem. Biol. Drug.,* **2007**, 70, 1–12.

[17] MO Taha; M Habash; Z Al-Hadidi; A Al-Bakri; K Younis; S Sisan, *J. Chem. Inf. Model.* **2011**, 51, 647–669.

[18] GM Morris; AJ Olson; DS Goodsell Protein–ligand docking methods, *Princ. Med. Chem.*, **2000**, 8, 31–48.

[19] Kontoyianni M; McClellan LM; Sokol GS*, J. Med. Chem.*, **2004**, 47, 558–565.

[20] C Beier; M Zacharias, *Expert Opin. Drug Dis.*, **2010**, 5, 347–359.

[21] S Boyd, FlexX suite, Chem. World UK .,**2007**, 4, 72.

[22] M Rarey; B Kramer; T Lengauer; G Klebe, *J. Mol. Biol.*, **1996**, 261, 470–489.

[23] TJA Ewing; S Makino; AG Skillman; ID Kuntz, *J. Comput. Aid Mol. Des.*, **2001**, 15,411–428.

[24] G Jones; P Willett; RC Glen; AR Leach; R Taylor, *J. Mol. Biol.*, **1997**, 267 ,727–748.

[25] M Vaque; A Ardrevol; C Blade; MJ Salvado; M Blay; J Fernandez- Larrea; L Arola; G Pujadas, *Curr. Pharm. Anal.*, **2008**, 4, 1–19.

[26] S Cosconati; S Forli; AL Perryman; R Harris; DS Goodsell; AJ Olson, *Expert Opin. Drug Dis.,* **2010**, 5, 597–607.

[27] GM Morris; DS Goodsell; RS Halliday; R Huey; WE Hart; RK Belew; AJ Olson*, J Comput Chem.*, **1998**, 19 ,1639–1662.

[28] TA Halgren; RB Murphy; RA Friesner; HS Beard; LL Frye; WT Pollard, *J. Med. Chem.*, **2004**, 47, 1750–1759.

[29] Accelrys Inc. Cerius2 LigandFit 4.10. Accelrys Inc.; San Diego, **2000**.

[30] DJ Diller; KM Merz , *Proteins* , **2001**, 43, 113–124.

[31] D Hecht; GB Fogel, *Curr. Comput. Aid Drug* , **2009**, 5, 56–68.

[32] C Bissantz; G Folkers; D Rognan, *J. Med. Chem.*, **2000**, 43, 4759–4767.

[33] WR Gao; YL Lai, *J. Mol. Model.*, **1998**, 4, 379–394.

[34] A Krammer; PD Kirchhoff; X Jiang; CM Venkatachalam; M Waldman*, J. Mol. Graph. Model*, **2005**, 23, 395–407.

[35] HFG Velec; H Gohlke; G Klebe, *J. Med. Chem.*, **2005**, 48, 6296–6303.

[36] AN Jain*, Curr. Protein Pept. Sci.*, **2006**, 7, 407–420.

[37] R Rajamani; AC Good, *Curr. Opin. Drug Disc.*, **2007**, 10, 308–315.

[38] EM Krovat; T Langer, *J. Chem. Inf. Comput. Sci.,* **2004**, 44, 1123–1129.

[39] PC Sharma; A Sinhmar; A Sharma; H Rajak; DP Pathak, *J. Enzyme Inhib. Med. Chem.* ,**2013**, 28 , 240-266.

[40] AS Girgis; HM Hosni; FF Barsoum, *Bioorg. Med. Chem.*, **2006**, 14 , 4466-4476.

[41] OM Memar; SK Tyring, *Int. J. Dermatal.*, **1995**, 34 , 597-606.

[42] KL Keller; NA Fenske, *J. American Acad. Dermatal.*, **1998**, 38 , 611-625.

[43] A Hoffer ; J Prousky, *Altern. Med. Rev.*, **2008**, 13, 287.

[44] E Cabrera-Rode; G Molina; C Arranz; M Vera; P González; R Suárez; M Prieto; S Padrón; R León; J Tillan; I García; C Tiberti; OM Rodríguez; A Gutiérrez; T Fernández; A Govea; J Hernández ; D Chiong; E Domínguez; U Di Mario; O Díaz-Díaz; O Díaz-Horta, *Autoimmunity* , **2006**, 39 , 333-340.

[45] P Franchetti; R Pasquelini; R Petrelli; M Ricciutelli; P Vita; L Cappellacci, *Biorg. Med. Chem.*, **2004**, 14, 4655-4658.

[46] W Shi; X Qian; RS Zhang; G Song*, J. Agric. Food Chem.,* **2001**, 49 , 124-130.

[47] L Labanauskas; E Udrenaite; P Gaidelis; A Brukstus, *Farmaco* ,**2004**, 59, 255-259.

[48] MA Al-Sha'er; MO Taha, *Med. Chem. Research*, **2011**, 21, 487-510.

[49] C Prodromou ; LH Pearl, *Curr. Cancer Drug Tar.*, **2003**, 3 , 301-323.

[50] MA Al-Sha'er , *Der Pharma Chemica* ,**2014**, 6 , 261-291.

[51] A Christopher; AK Boris; SJ Brian, *Bioorg. Med. Chem.,* **2006**, 14, 1134–1142.

[52] Y Xu; Q Zhu; D Chen; Z Shen; W Wang; G Ning; Y Zhu, *Tumour Biol* , **2015** [in Press].

[53] MA Al-Sha'er; MO Taha, *J. Mol. Modeling*, **2012**, 18, 4843-4863.

[54] MA Al-Sha'er; MO Taha, *J. Chem. Inf. Model.*, **2010**, 50, 1706-1723.

[55] CERIUS2 4.10 LigandFit User Manual; Accelrys Inc.: San Diego; CA, **2000**.

[56] CERIUS2 QSAR Users' Manual; version 4.10; *Accelrys* Inc.: San Diego; CA, **2005**; 43–88; 221–235; 237-250.

[57] CM Venkatachalam; X Jiang; T Oldfield; M Waldman., *J. Mol. Graphics Modell.*, **2003**, 21 289–307.